ADVANCES IN FOREST FIRE RESEARCH

2022

Edited by

DOMINGOS XAVIER VIEGAS
LUÍS MÁRIO RIBEIRO

Factors Influencing Ember Accumulation Near a Building

Stephen L. Quarles[1]; Christine Standohar-Alfano[2]; Faraz Hedayati[1], Daniel J. Gorham*[1]

*[1] Insurance Institute for Business & Home Safety. 5335 Richburg Rd, Richburg, SC 29729, USA,
{steveq0629@gmail.com}, {fhedayati, dgorham}@ibhg.org
[2] Haag Engineering. 2224 E. 117th St, Burnsville, MN 55337, USA, {Christine.Standohar@gmail.com}*

*Corresponding author

Abstract

Embers, also known as firebrands, are the leading cause of building ignition during wildland-urban fires. This is attributed to direct ignitions of materials on, in, or attached to the building, and indirect ignition when they ignite vegetation or other combustible material near the building which can result in radiant heat and / or direct flame contact that ignites the building. Where and when embers accumulate near a building and ignitable fuel presents the potential for indirect ember ignition of the building. Factors that influence ember accumulation near a building include building geometry, such as flat wall and re-entrant corners, building wind angle, wind speed and the surface roughness characteristics of the horizontal landscape close to the building. Experiments conducted at the Insurance Institute for Business & Home Safety (IBHS) Research Center, using full-scale buildings with the above-mentioned factors provided a means to quantify ember accumulation on a mass per unit area basis.

1. Introduction

One of the main challenges to combating wildfires is that they spread through three main mechanisms, including flame impingement, radiant heat, and wind-blown embers, also referred to as firebrands. Ignition of a structure can be caused by direct flame contact from the primary fire front or from fires caused by localized fuel sources (i.e. vegetation, fences, etc.) near the structure (Potter and Leonard 2010, Quarles et al. 2010). Regardless of the source of the flame, ignition of the exterior of the building can result in ignition of internal contents. Buildings near flames are subjected to radiant heat and their vulnerability depends on both the intensity of the radiation as well as the duration (Potter and Leonard 2010).

The third mechanism of wildfire spread is by exposure to embers. This mode is the most important cause and accounts for up to 90% of structural ignitions (Potter and Leonard 2010). For example, two of every three homes destroyed in the 2007 Witch Creek fire in San Diego County, CA were ignited by ember accumulation (Quarles et al. 2010). The risk of ignition from embers depends on several features, including the number of embers, the ember characteristics, the amount of and type of combustible debris or materials near the building, duration of the ember attack, and environmental conditions. In some cases, ember attacks can result in the ignition of a building 12 hours after the initial fire front passes (Potter and Leonard 2010). The delayed ignition can be explained by either the continued production of embers from burning fuels after the fire front passed, or the smoldering combustion of a component or assembly that eventually transitioned to flaming combustion.

The lifecycle of embers that cause destruction of homes and building can be described in three stages: 1) production and release of embers from burning fuel; 2) transport of embers from the source to where they are deposited, including accumulation; and given sufficient accumulation and receptive fuel 3) ignition. Given the dominant role that embers play in wildfire spread and home ignition (Manzello et al. 2020) a considerable amount of research has been conducted and is underway on this topic. Experiments conducted by Suzuki and Manzello (2017) also studied accumulation zones created by stagnation planes in front obstacles. These investigations found that wind speed (6, 8, and 10 m/s) influenced the accumulation of firebrands in the stagnation plane on the windward side of obstacles and suggest experiments at wind speeds greater than 10 m/s would be desirable. In the stagnation zone roughness of horizontal surface affects the accumulation of embers (Suzuki & Manzello 2017). Later work investigated the effect of structure separation distance on firebrand

accumulation (Suzuki and Manzello 2021) which highlighted the role of firebrand behaviour between two structures. The heat flux, and ignition potential, from a pile of accumulated embers is distinctly different than from an individual ember (Hakes et al. 2019).

Nguyen and Kaye (2022) conducted a series of small-scale wind tunnel experiments investigating non-combustible ember accumulation on building rooftops and found that building geometry and wind angle were important factors for accumulation rates. Separate from and prior to these previous studied a set of experiments were conducted at IBHS to study the accumulation of embers near a building as a function of wind speed, building geometry, and wind angle. This work is the focus of the present paper.

2. Methodology

These ember accumulation experiments were conducted as part of the 2015 wildfire experimental campaign at the IBHS Research Center in Richburg, South Carolina. This research facility includes a wind tunnel large enough to hold full-scale one- and two- story residential and small commercial buildings, allowing for investigations to evaluate the performance of buildings subjected to high winds (Standohar-Alfano et al. 2017). The facility is able to generate wind speeds greater than 71.5 m/s (100 mph) using a 105-fan array. The wind tunnel can generate a constant wind speed or replicate observed, fluctuating wind records from hurricanes, thunderstorms, or open country conditions. For the 2015 wildfire experimental campaign, an open country wind record was used and was scaled to generate wind time histories defined as medium and high. The medium and high wind speed traces were fluctuating records with an average wind speed of 10.3 and 17.4 m/s (23 and 39 mph), respectively. Figure 1 shows the medium and high wind speed traces used in the experiments. In addition, an idle fan speed was used which ranged between 4.5-5.4 m/s (10-12 mph).
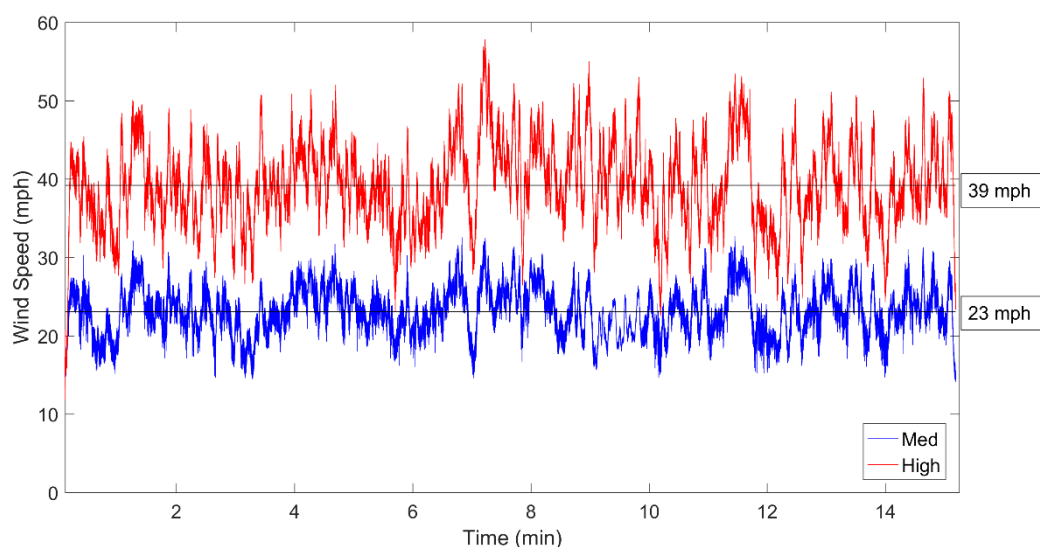
Figure 1. Medium and high wind speed records used in the 2015 wildfire experimental campaign (1 mph = 0.45 m/s). The average wind speeds for the "medium" and "high" wind speeds are boxed to the right of the respective record.

The wind tunnel utilizes a large turn table with a radius of 16.8 m (55 ft) which can rotate 360°, allowing for the full rotation of the test building and therefore the evaluation of the effect of wind speed and direction on the deposition of embers around the test building.

The 2015 wildfire experimental campaign used a custom-made system to deliver fuel and generate embers. The fuel was a mixture of southern yellow pine wood chips and wooden dowels processed from midwestern hardwood species, with a ratio of 80% and 20%, by weight, respectively. All raw material was dried to a moisture content less than 10%. The generators were used to burn fuel and create embers, as shown in Figure 2. The fuel was delivered into the generator by the auger feed line shown by Figure 2A. The fuel dropped on top of a metal grate immediately above a gas burner (not shown). A fan located under the burner (Figure 2B) pushed embers up and out of the exhaust chute indicated by Figure 2C. Eight generators were placed at equally spaced increments in front of the fan array.
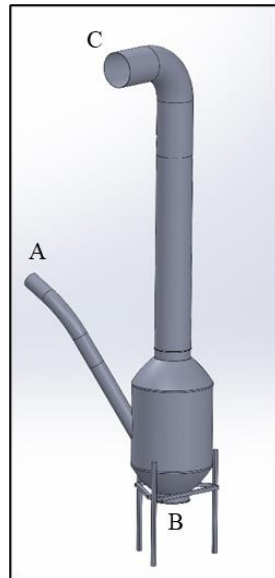
Figure 2. Schematic of the ember generators used. A is the auger feed line which introduced the fuel into the generator; B is the location of the vertically oriented fan; and C is the exhaust chute.

An overview of the auger system, generators, and test building is shown in Figure 3. Prior to testing, fuel was placed in the hoppers shown in Figure 3A. Five augers (not shown) dropped fuel into the pneumatic feed lines. The feed rate was controlled by powering the augers on and off. The desired feed rate was obtained when individual augers were turned on for a predetermined length of time between 3-5 seconds and then off for 10-20 seconds. Establishing the on/off times for each individual auger was determined based on visual inspection of ember output and observed overheating of the generators. The goal of using the intermittent fuel delivery was to ensure a consistent output of embers by all generators without damaging the generators from excessive heat.
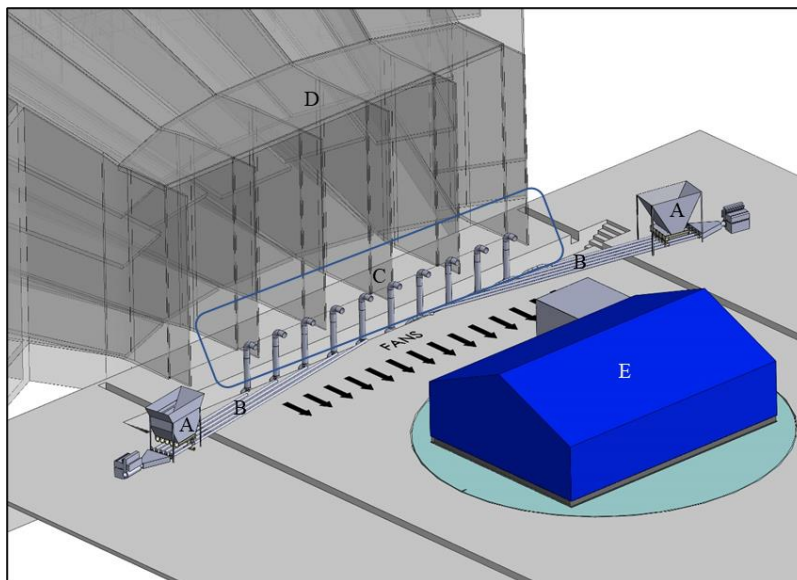
Figure 3. Experimental setup, including auger feed and ember generator system. The left and right hoppers are shown in A; B indicates the auger feed lines which deliver fuel to the 10 generators indicated in C; D is the fan array behind the generators; and E is the test building.

The auger delivered fuel to feed lines shown as B in Figure 3. These feed lines delivered the fuel to the generators (Figure 2A and Figure 3C). As described earlier, the generators burned the fuel and a fan pushed embers up the exhaust chute. Using the wind traces shown in Figure 1, the fan array (Figure 3D) created the wind flow in the test chamber. The test building shown by E in Figure 3 was then subjected to an ember exposure. The duration of the exposure was 15-minutes. The system used in this study is shown in Figure 4. By placing a building in the wind field and exposing it to embers, embers were collected at various near-building locations.

Figure 4. Test building and ember generator system used in the accumulation study. As shown, the collection trays were initially covered with a solid panel until steady flow from the generators was observed.

To evaluate ember accumulation in the vicinity of a building, a full-scale structure was positioned in the wind tunnel (Figure 3E and Figure 5). The structure was one-story with a building footprint of 9.1 m x 12.2 m (30 ft x 40 ft). To evaluate the vulnerability of a re-entrant corner, a 3 m x 3 m (10 ft x 10 ft) cube was placed on one corner of the long axis, as shown in Figures 4 and 5. This cube detached and re-attached at different locations on the test building. The building and cube were clad with fiber-cement panels. The orientation of the building was varied to assess the impact of wind direction on ember accumulation.
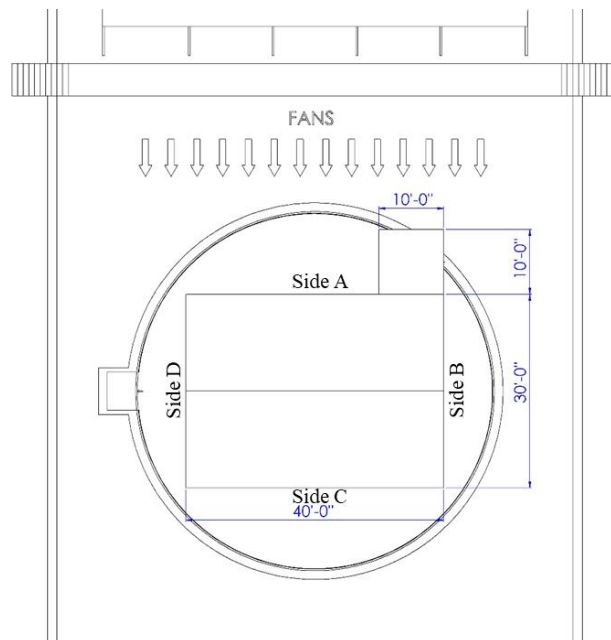
Figure 5. Plan view of the test building used in the accumulation experiments.

2.1. Ember Accumulation and Characterization

For the ember accumulation portion of the experiments, water-filled pans were placed at various locations on the test building. The building was then subjected to an ember exposure for 15 minutes. Thirteen scenarios were

examined at both medium and high wind speeds, as shown in Table 1. With the exception of the 270 orientation, a water-filled pan was placed in the re-entrant corner. Two additional water-filled pans (defined as WP 1 and WP 2) were positioned at selected locations along the building, as indicated in Table 1. Location information is also provided in Figure 6.

Table 1. Ember Accumulation Test Matrix.

Orientation	Pan Corner	WP 1	WP 2
0°A	Yes	1.5 m (5 ft)	1.5 m (5 ft)
15°A	Yes	1.5 m (5 ft)	1.5 m (5 ft)
330°B	Yes	0 m (0 ft)	0 m (0 ft)
345°B	Yes	0 m (0 ft)	0 m (0 ft)
0°B	Yes	0 m (0 ft)	0 m (0 ft)
15°B	Yes	0 m (0 ft)	0 m (0 ft)
30°B	Yes	0 m (0 ft)	0 m (0 ft)
60°	Yes	0 m (0 ft)	3.8 m (12.5 ft)
75°	Yes	0 m (0 ft)	3.8 m (12.5 ft)
90°	Yes	0 m (0 ft)	3.8 m (12.5 ft)
105°	Yes	0 m (0 ft)	3.8 m (12.5 ft)
120°	Yes	0 m (0 ft)	3.8 m (12.5 ft)
270°	No	1.5 m (5 ft)	3.1 m (12 ft)

As indicated in Table 1, there were four main parent orientations investigated, shown in bold (0°A, 0°B, 90°, and 270°). With these four scenarios, the face closest to the fans was perpendicular to the wind field. For three of the main orientations (0°A, 0°B, and 90°) the re-entrant corner was directly impacted by the wind field (i.e., not on the leeward side of the building). In order to assess the impact of wind direction on ember accumulation the building was rotated in 15° increments. The location of the re-entrant corner on the test building was assessed with two of the main orientations (0°A and 0°B). For scenarios with an A orientation, the cube was in its original location at the end of the building as indicated in Figure 5. For the cases with a B orientation, the cube was moved to the mid-length of the building (centered at 6.1 m (20 ft)).

The pan location is also included in Table 1. The corner pan was located in the re-entrant corner and there was only one orientation where it was not utilized. There were two wall pans (WP 1 and WP 2) used in the ember accumulation experiments. The location is given as the distance from the closest corner. For the A scenarios, both pans were placed 1.5 m (5 ft) from the corners of the windward side. For the B scenarios, both of the wall pans were placed at the corner (0 m). For the cases where the main (parent) orientation was 90°, one pan was placed at the corner and the second pan was placed 3.8 m (12.5 ft) from the same corner. This resulted in a spacing of 2.3 m (7.5 ft) between the pans. For the 270° orientation, one pan was placed 1.5 m (5 ft) from one corner and the second pan was placed 3.1 m (12 ft) from the other corner.
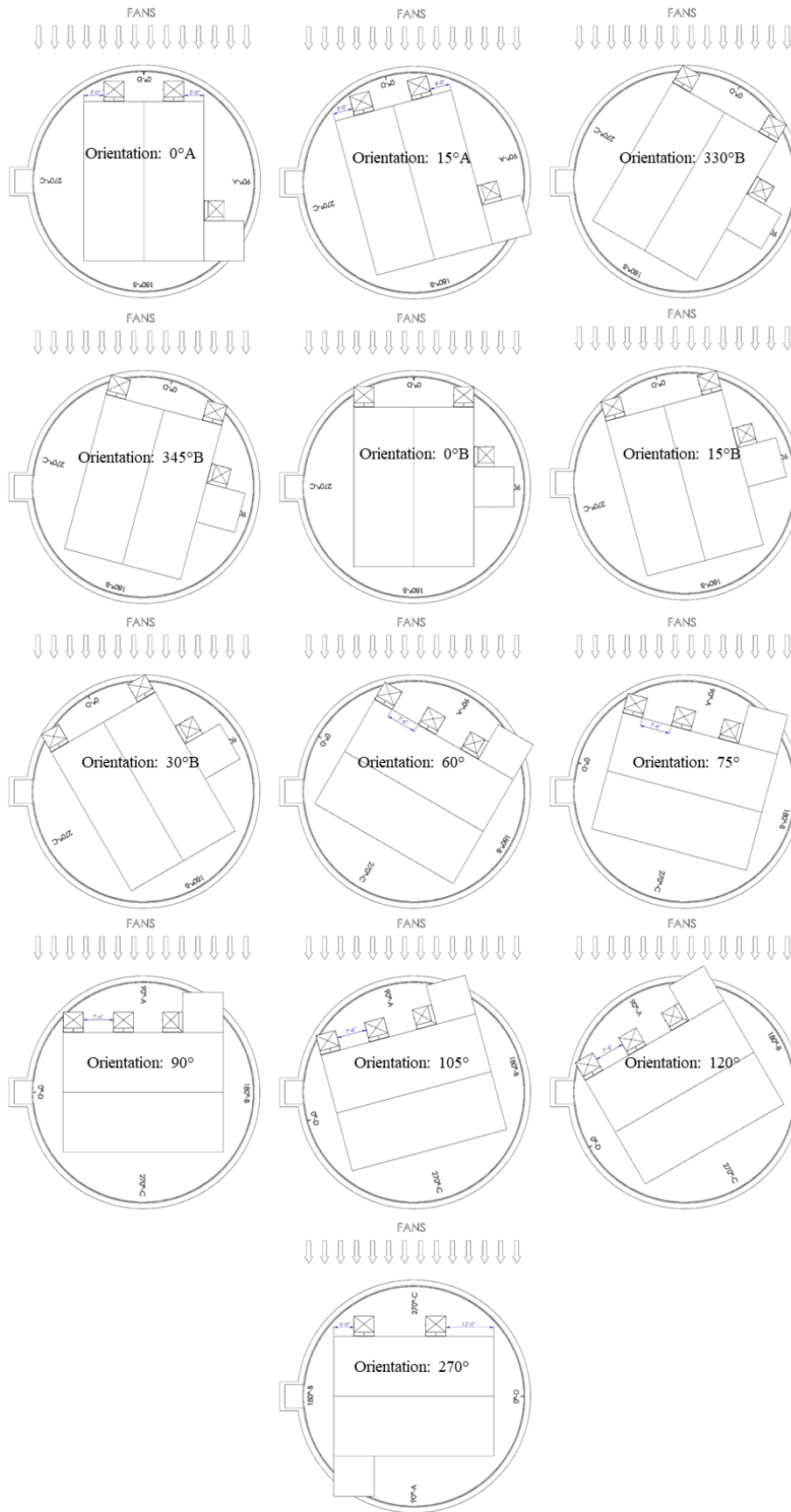
Figure 6. Pan location for all orientations.

At the beginning of each test, during the time the generators were starting up and output was non-uniform, the pans were covered. Once the generators reached a steady state the cover was removed and the wind speed record began, marking the start of the 15-minute exposure. The orientations summarized in Table 1 were subjected to both the medium and high wind speed traces.

The water-filled pans used in the ember accumulation study measured 1.5 m x 1.5 m (5 ft x 5 ft) and were divided into two sections defined as field and wall. The wall section was the area closest to the exterior wall. For all pans, this was 0.3 m (1 ft) from the wall edge. The field section was larger than the wall section and was the remaining portion of the water-filled pan that was not immediately adjacent to the building. Figure 7 shows an image of the two types of pans used in the accumulation study. Figure 7a illustrates the pan that was placed in the re-entrant corner. Since this pan had two edges against a wall, the wall section was larger than the pans placed elsewhere on the building.
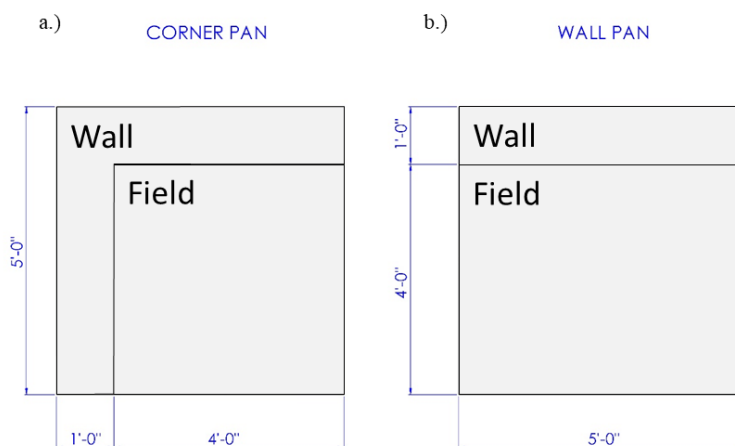
Figure 7. Water-filled pan dimensions and sections where a.) is the pan at the re-entrant corner and b.) is the pan placed along the flat wall (WP 1 and WP 2).

In addition to estimating the ember accumulation in the water-filled pans, the mass and surface area of individual embers was also measured. This was done to study the variability in ember characteristics. The surface area was calculated using image processing software and the mass was found using a high-precision electronic scale.

3. Results and Discussion

Results from the accumulation study are shown in Figures 8 through 11. There was variability in the accumulation depending on orientation, wind speed, pan section (wall or field), and pan placement along the wall of the test building. Thirteen orientations were investigated. The orientation of the test building with Side A facing the fans, as shown in Figure 5, was designated as the 90°orientation. Side B was designated 180°, Side C was designated 270° and Side D was designated 0°.

The results for the 270°orientation are shown in Figure 8. This was the only orientation that was tested at the idle (non-fluctuating) wind speed. This orientation positioned the cube on the leeward side of the building, so no embers were collected in the corner pan. The results for this orientation indicated that maximum ember accumulation occurred in the wall sections. At this orientation, the difference in accumulation between the wall and field sections increased with increasing wind speed.
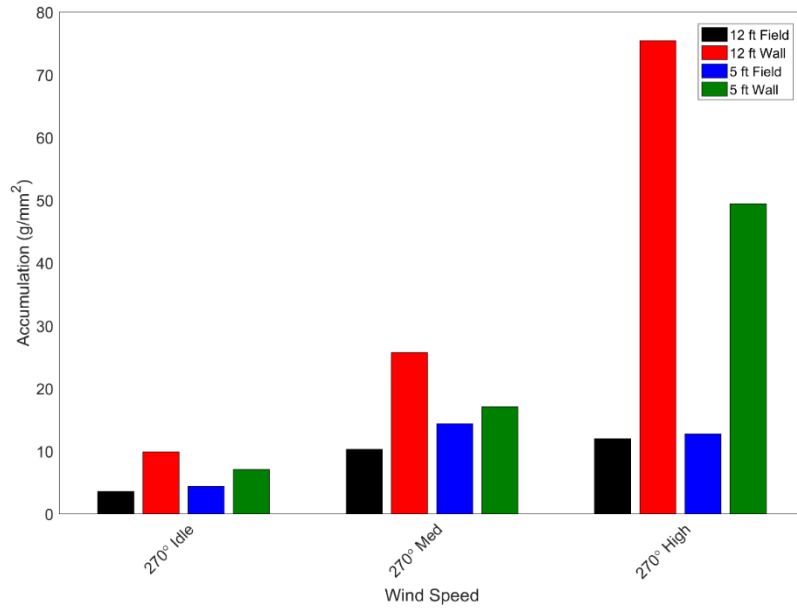
Figure 8. Ember accumulation in water-filled pans. The length direction of the test building faced the fans.

For the orientations in the 90° parent orientation (Figure 9), the 60° had the highest accumulation for both the medium and high wind speeds. At this orientation, WP 1 and WP 2 were closer to the ember generators and the re-entrant corner was positioned so that embers were naturally caught in the corner pan. For this reason, accumulation values were relatively high. At 105° and 120°, ember accumulation decreased. For these orientations, the cube used to simulate the re-entrant corner did provide some shelter for locations on the leeward side of the cube where the water-filled pans were placed.
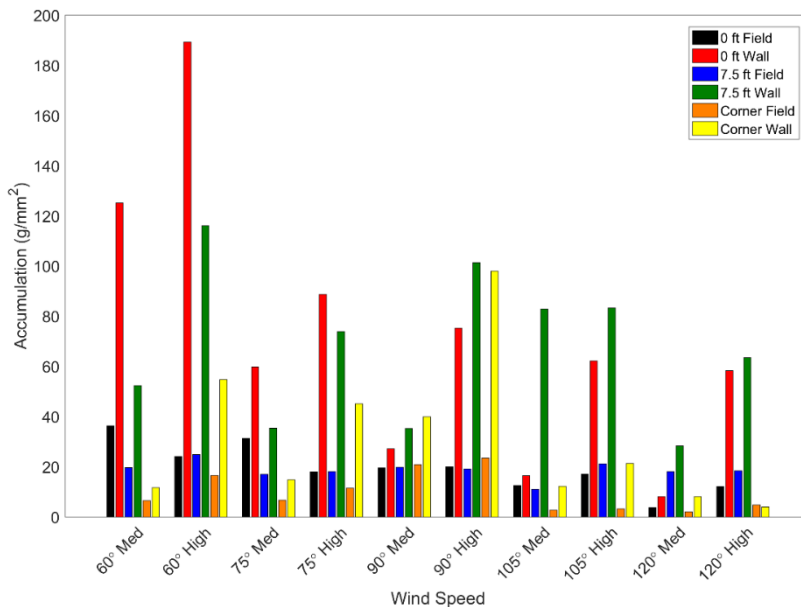
Figure 9. Ember accumulation in water-filled pans. Results are presented for the 90° parent orientation.

The results of accumulation for the 0°A and 15°A orientation is shown in Figure 10. As with previous orientations, the wall section of the pans had higher accumulations than the field sections for a given wind speed. Likewise, the high wind speed record did result in higher values of accumulation. Since the re-entrant corner was located 9.1 m (30 ft) from the windward edge of the building, ember accumulation in the corner pan was minimal due to the distance from the ember generators.
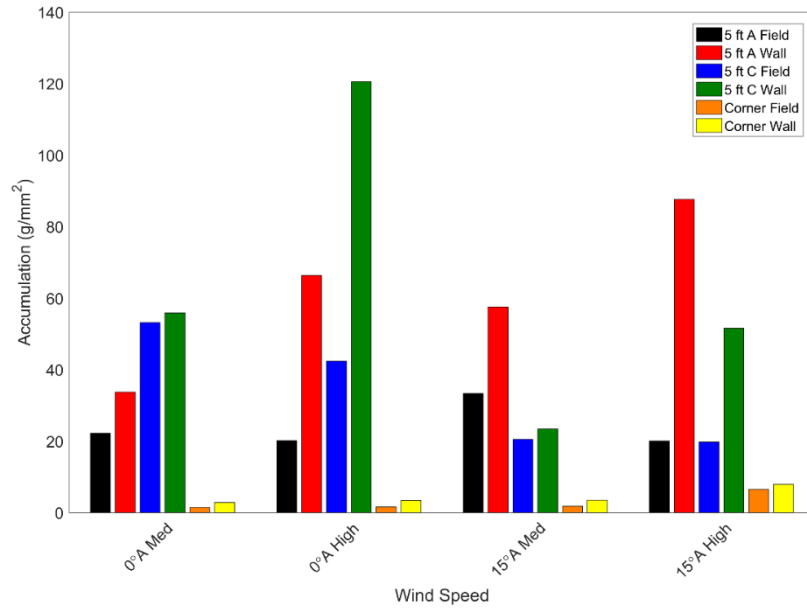
Figure 10. Ember accumulation in water-filled pans. Results are presented for the 0°A parent orientation.

Finally, the results of the 0°B parent orientation are shown in Figure 11. For these orientations, the re-entrant corner was located at the mid-span of the test building and was closer to the ember generators. As with other orientations, the wall section of the water-filled pans saw larger values of ember accumulation as compared to the field section. Likewise, high wind speeds typically resulted in higher values of accumulation. The 330°B and 345°B orientations had higher accumulations in the water-filled pan located on the C side of test building. With these orientations, the test building was rotated such that the C side was closer to the generators, so this result was not surprising. Similarly, for the 15°B and 30°B orientation, the A side of the building was closest to the generators, so accumulation was greatest in the water-filled pan located on the A side of the windward wall. Likewise, as the test building was rotated counter-clockwise from 0°B, the re-entrant corner moved closer to the generators and there was an observed increase in ember accumulation at the corner pan.
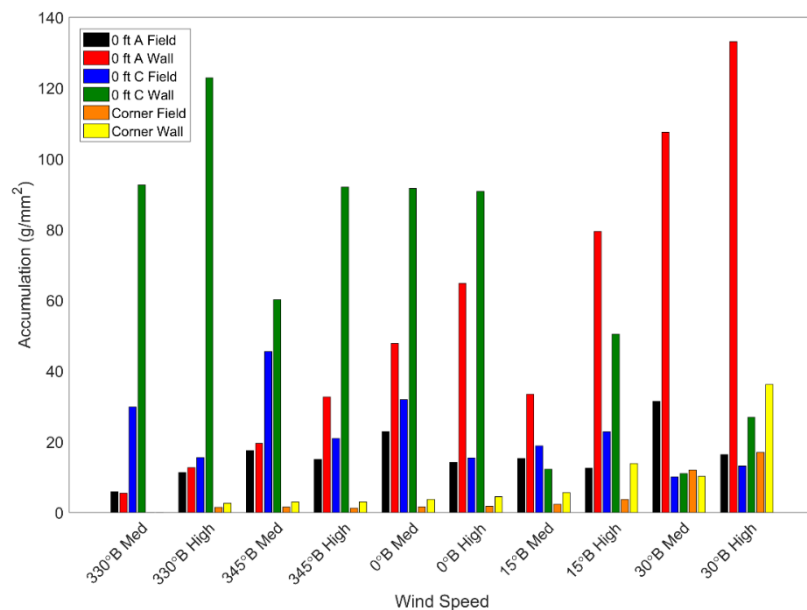
Figure 11. Ember accumulation in water-filled pans. Results are presented for the 0°B parent orientation.

In addition to quantifying ember accumulation, characterization of individual embers was also performed by measuring mass and surface area. The goal of this portion of the work was to add to the knowledge base regarding the quantification of ember exposure since this is an area of needed research. Due to the large number

of orientations investigated, only embers from the four parent orientations (270°, 90°, 0°A, and 0°b) were included.
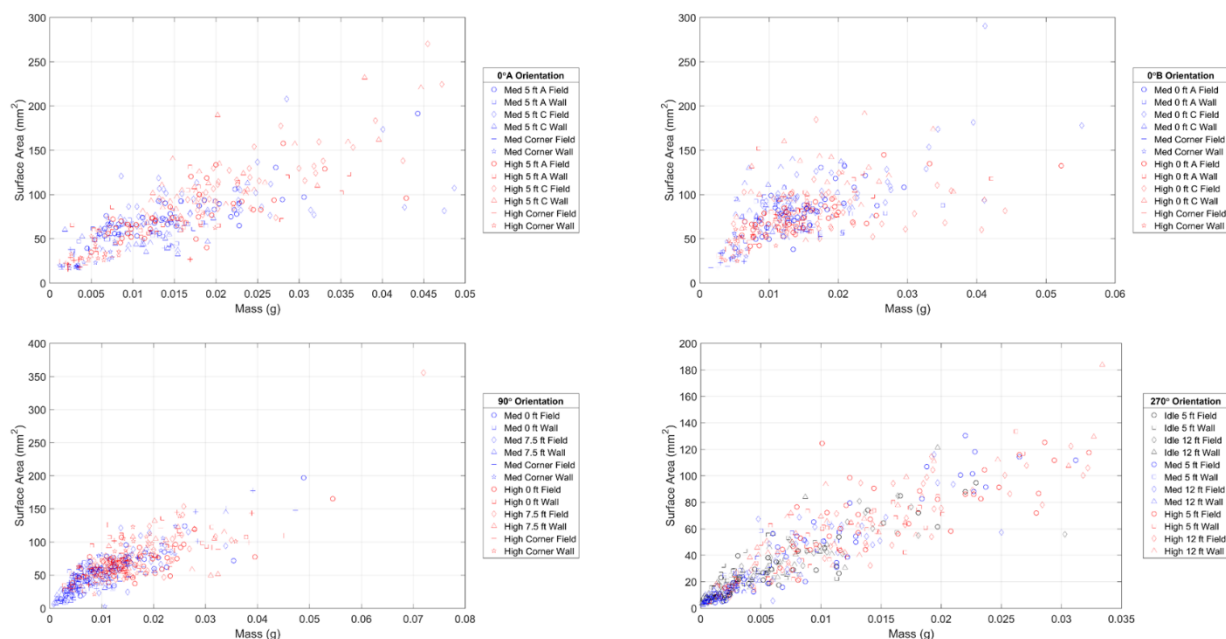
Figure 12. Ember characteristics, mass and surface area, from ember generators and collected in water-filled pans.

The relationship between mass and surface area is relatively linear and as the surface area increases, so does the mass. There did not appear to be any strong dependency between wind speed and ember surface area or mass. Likewise, the orientation did not appear to have an important impact on ember surface area or mass. This was not surprising since fuel type plays a larger role in ember characteristics than building orientation. As data regarding ember characteristics from active wildfires becomes available, a comparison can be made to the embers created with the IBHS generators. Using that information, the generators and/or fuel can be modified to better replicate embers collected in the field.

4. Conclusion

Overall, the data suggested that the accumulation for the wall section was higher than the accumulation for the field section, thus indicating greater vulnerability at locations immediately adjacent to the building. For the wall sections, higher wind speeds resulted in greater accumulation. Higher wind speeds allowed more embers to reach the building and become caught in the recirculation where they were forced into the water-filled pans. For the field sections, accumulation values were typically largest for the medium wind speed record, however, the dependency of accumulation on wind speed was lower. This likely resulted in the relatively large size of the field section, so at medium wind speed, lower momentum embers could land directly in the field section since they were unable to reach the building.

These results have important implications, especially for rough ground surfaces immediately adjacent to buildings. If embers strike a building and become contained in the recirculation, they can be forced down to the ground. If the ground surface is rough (i.e., mulch), it will capture the embers and allow them to accumulate closer to the building. Any combustible material near accumulated embers can potentially ignite which would result in direct flame contact or elevated levels of radiant heat near a building.

5. References

Manzello SL, Suzuki S, Gollner MJ, Fernandez-Pello, AC (2020) Role of firebrand combustion in large outdoor fire spread. Progress in Energy and Combustion Science. doi: 10.1016/j.pecs.2019.100801

D. Nguyen, N.B. Kaye, Quantification of ember accumulation on the rooftops of isolated buildings in an ember storm, Fire Saf. J. 128 (2022), https://doi.org/10.1016/j. firesaf.2022.103525.

Potter M and Leonard J (2010). Spray System Design for Firebrand Attack – Research Findings and Discussion Paper. CSIRO – Sustainable Ecosystems, Report No. EP103159, 1-27.

Standohar-Alfano CD, Estes H, Johnston T, Morrison MJ, Brown Giammanco TM (2017) Reducing losses from wind-related natural perils: research at the IBHS Research Center. Frontiers in Built Environment 3, 9. doi:10.3389/FBUIL.2017.00009

Suzuki S and Manzello SL (2017) Experimental investigation of firebrand accumulation zones in front of obstacles. Fire Safety Journal. doi: 10.1016/j.firesafe.2017.08.007

Manzello, S.L.; Suzuki, S.; Gollner, M.J.; Fernandez-Pello, A.C. The role of firebrand combustion in large outdoor fire spread. Prog. Energy Combust. Sci. 2020, 76, 100801.

Suzuki S and Manzello SL (2021) Investigating the Effect of Structure to Structure Separation Distance on Firebrand Accumulation. Front. Mech. Eng 6:628510. doi: 10.3389/fmech.2020.628510

Quarles, Stephen L., Valachovic, Yana, Nakamura, Gary M., Nader, Glenn A., and De Lasaux, Michael J, (2010). Home Survival in Wildfire-Prone Areas: Building Materials and Design Considerations. University of California Agriculture and Natural Resources. ANR Publication 8393.